Adenovirus Type 37 Keratitis in the C57BL/6J Mouse

Ashish V. Chintakuntlawar,[1,2] *Roger Astley,*[1] *and James Chodosh*[1,2,3]

Purpose. To develop a mouse model of adenoviral keratitis that will allow further study of viral and host pathogenic mechanisms.

Methods. Corneas of C57BL/6J mice were injected with adenovirus type 37 (Ad37) or virus-free dialysis buffer by a gas-powered microinjection system coupled to a glass micropipette needle. Mouse corneas were examined for signs of inflammation, by clinical examination, immunohistochemistry, and confocal microscopy; assayed for viral and chemokine mRNA expression by real-time PCR; titered to assess viral replication; and subjected to ELISA for chemokine and myeloperoxidase (MPO) protein expression.

Results. C57BL/6J mice corneas injected with 10^5 TCID (tissue culture infective dose) Ad37 showed stromal opacification and inflammation beginning from 1 day after injection and continuing for several months, while buffer-injected corneas showed no signs of inflammation. Ad37-injected corneas expressed adenoviral E1A 10S and E1B 19k mRNA but not IIIa, and viral titers had fallen two logs by day 4 after injection. When compared to untouched and buffer-injected corneas, Ad37-injected corneas expressed significantly higher levels of IL-6, KC, and MCP-1 mRNA at 4 hours after injection ($P < 0.05$). By ELISA, KC protein was significantly elevated in Ad37-injected corneas at 8 and 16 hours, and MCP-1 protein at 16 hours after injection ($P < 0.05$). Ad37-injected corneas showed elevated levels of MPO ($P = 0.0024$) at 4 days after injection consistent with immunohistochemical evidence for a predominance of neutrophils in the corneal stroma.

Conclusions. Ad37 induces an acute immunopathologic response in the C57BL/6J mouse cornea, despite an absence of viral replication. This new animal model of Ad37 keratitis will facilitate studies of the molecular pathogenesis of the disorder. (*Invest Ophthalmol Vis Sci.* 2007;48:781–788) DOI:10.1167/iovs.06-1036

Adenoviruses were discovered over 50 years ago by Rowe et al.[1] and Hilleman et al.,[2] and are medium sized, 60 to 90 nm in diameter, nonenveloped, and icosahedral shaped, with a linear double-stranded DNA genome. Adenoviruses infect a wide range of organisms across the vertebrate animal world from fish to humans,[3] but exhibit strict species specificity. For example, human adenoviruses do not typically infect other animals,[4] but in humans they induce significant and relatively common infections of the respiratory, gastrointestinal, and genitourinary tracts[5] and fatal disseminated infections in the immunocompromised host.[6] Three common ocular adenovirus syndromes have been described: follicular conjunctivitis, pharyngoconjunctival fever, and epidemic keratoconjunctivitis (EKC), the latter caused principally by the species D adenoviruses Ad8, Ad19, and Ad37.[7] EKC is a highly contagious acute infection of the ocular surface and is the only adenoviral ocular syndrome that significantly involves the cornea. EKC is associated with chronic and recurrent, multifocal, leukocytic infiltration of the subepithelial cornea, a pathognomic feature of the infection that may cause significant morbidity.[8,9]

Previous in vitro and in vivo data have shown that adenoviruses can induce host cell chemokine expression and inflammation in the absence of viral replication.[10–13] Keratocytes, the resident cells of the corneal stroma, play a major role in innate immune responses to corneal infection by producing inflammatory cytokines and chemokines.[14–18] In vitro studies performed with cultured keratocytes have shown that expression of chemokines involves adenovirus binding to the host cell and subsequent activation of signaling molecules, including c-Src and mitogen-activated protein (MAP) kinases. The expression of chemokines in these cells can be inhibited with specific pharmacologic signaling inhibitors.[12,19]

The role of corneal cells in the molecular pathogenesis of adenovirus keratitis has not been extensively investigated in vivo due to the species specificity of human adenoviruses. Existing animal models of adenoviral ocular infection, such as the cotton rat,[20] New Zealand White rabbit,[13,21] and Hollander rabbits[22] are not amenable to genetic manipulation and thus are not optimally suited for the study of adenoviral pathogenesis. We report for the first time the successful infection of the C57BL/6J mouse cornea with human Ad37, and describe subsequent chemokine expression and immunopathologic responses. This new mouse model of adenovirus keratitis should allow studies of adenoviral pathogenesis that have not been possible.

Materials and Methods

Virus and Animals

Eight to 12-week-old female C57BL/6J mice were purchased from Jackson Laboratories (Bar Harbor, ME) and were treated according to the ARVO Statement for the Use of Animals in Ophthalmic and Vision Research. Human Ad37 was obtained from American Type Culture Collection (ATCC, Manassas, VA). Virus stock was prepared by infecting A549 cells (ATCC) in minimum essential medium (Invitrogen, Carlsbad, CA), supplemented with 2% fetal bovine serum, penicillin G sulfate, and streptomycin, followed by cesium-chloride gradient purification and dialysis.

Experimental Infections

C57BL/6J mice were anesthetized by intramuscular injection of ketamine (85 mg/kg) and xylazine (14 mg/kg). Anesthetic drops (0.5% proparacaine hydrochloride, Alcon, Fort Worth, TX) were also applied topically to each eye before injections. One microliter of Ad37 (10^1–10^5 TCID [tissue culture infective dose]) or virus-free dialysis buffer was injected in the right central corneal stroma with a glass micropipette needle fitted with a gas-powered microinjection system (MDI,

From the Molecular Pathogenesis of Eye Infection Research Center, Dean A. McGee Eye Institute, and the Departments of [1]Ophthalmology, [2]Cell Biology, and [3]Microbiology and Immunology, University of Oklahoma Health Sciences Center, Oklahoma City, Oklahoma.

Supported by US Public Health Service Grants R01 EY13124 and P30 EY12190 and a Physician-Scientist Merit Award (to JC) from Research to Prevent Blindness, New York, New York.

Submitted for publication September 1, 2006; revised October 5, 2006; accepted December 14, 2006.

Disclosure: **A.V. Chintakuntlawar**, None; **R. Astley**, None; **J. Chodosh**, None

The publication costs of this article were defrayed in part by page charge payment. This article must therefore be marked "*advertisement*" in accordance with 18 U.S.C. §1734 solely to indicate this fact.

Corresponding author: James Chodosh, DMEI-OUHSC, 608 Stanton L. Young Blvd., Oklahoma City, OK 73104; james-chodosh@ouhsc.edu.

TABLE 1. Primer Sequences and GenBank Accession Numbers for Real-Time PCR

Gene	Primer Sequence	GenBank* Accession No.
E1A 10S	FP 5′ GGAGGTAGATGCCCATGATGA 3′ RP 5′ GTTGGCTATGTCAGCCTGAAGA 3′	AF099665
E1B 19k	FP 5′ GTGGACTATCCTTGCAGACTTTAG 3′ RP 5′ TTCCAAACCAGTGTCTCCAGAAC 3′	AF099665
IIIa	FP 5′ CCTTTCCTAGCTTAGGGAGTT 3′ RP 5′ CGAGTCGTTCAGGTACTCGTC 3′	AF108105
IL-6	FP 5′ CACAGAGGATACCACTCCCAACA 3′ RP 5′ CATTTCCACGATTTCCCAGAGA 3′	NM_031168
KC	FP 5′ GCGCCTATCGCCAATGAG 3′ RP 5′ AGGGCAACACCTTCAAGCTCT 3′	U20527
MCP-1	FP 5′ GCCCTAAGGTCTTCAGCACCTT 3′ RP 5′ TGCTTGAGGTGGTTGTGGAA 3′	AF065931
GAPDH	FP 5′ GACAATGAATACGGCTACAGCAACAGG 3′ RP 5′ GTTGGGATAGGGCCTCTCTTGCTCA 3′	BC083080

FP, forward primer; RP, reverse primer.
* http://www.ncbi.nlm.nih.gov/Genbank; provided in the public domain by the National Center for Biotechnology Information, Bethesda, MD.

South Plainfield, NJ) under an ophthalmic surgical microscope (Carl Zeiss Meditec, Inc., Thornwood, NY). Left eyes were untouched. At indicated time points after injection, mice were euthanized using CO_2 inhalation and both corneas removed and placed in RNA stabilizer (RNALater; Ambion, Austin, TX) for RNA studies or phosphate-buffered saline (PBS) for protein studies.

RNA Isolation and Reverse Transcription

Untouched, buffer-injected, and Ad37-injected corneas (three for each group) were used in each experiment. Total RNA was isolated by the single-step RNA isolation method (TRIzol; Invitrogen) performed according to instructions provided by the manufacturer. Contaminating genomic DNA was removed from total RNA with DNase treatment (Ambion). The quality and concentration of RNA was determined using spectrophotometry. Two micrograms of total RNA isolated from each group was reverse transcribed to yield single stranded cDNA using 200 U Moloney murine leukemia virus (MMLV) reverse transcriptase, 2 mM dNTPs, 20 U of recombinant RNasin and 5 ng of oligo(dT) 15mer (all from Promega, Madison, WI) as primer in a total reaction volume of 20 μL. Samples without MMLV reverse transcriptase were used in control experiments, to rule out genomic DNA contamination. The reaction mix was incubated at 25°C for 5 minutes, then at 37°C for 1 hour, followed by enzyme inactivation at 72°C for 15 minutes.

Real-Time PCR

A total of 2 μL of cDNA obtained by reverse transcription was used for amplification in a final volume of 20 μL containing 10 μL of 2× SYBR green master mix (Applied Biosystems [ABI], Foster City, CA) and 250 nM of specific forward and reverse primers. RNA concentrations of samples were normalized using quantification of GAPDH mRNA as the internal control. Quantitative real-time PCR amplification was performed (ABI Prism 7000 Sequence Detection System; PE Applied Biosystems) according to the manufacturer's instructions. Dissociation curves were analyzed for generation of a single product. Relative transcript levels were calculated according to the formula $1000 \times 2^{-\Delta Ct}$, where ΔCt equals $Ct_{\text{gene of interest}} - Ct_{\text{internal control}}$. Reaction mixtures lacking template and cDNA prepared without reverse transcriptase were used as the control in all experiments. Primers for real-time PCR were designed on computer (Primer Express Software; ABI). All primers were checked for efficiency, and only primers with equal efficiency were used in the experiments. Because the Ad37 sequence is currently unknown, primers for viral genes were designed with the known sequences of Ad9 and Ad17, also species D adenoviruses. Primer pairs used in these experiments are shown in Table 1.

Viral Replication Assay

C57BL/6J mouse corneas injected with 10^5 TCID of Ad37 ($n = 4$/time point) were removed, homogenized in 250 μL of 2% MEM, freeze-thawed, centrifuged at 10,000*g* for 10 minutes, and the supernatants titered in triplicate in A549 cells.

Cy3 Labeling of Ad37

Viral particle concentration was determined based on the viral sample's absorbance at 260 nm. Ad37 was then conjugated with Cy3 dye (GE Healthcare, Piscataway, NJ) as per Leopold et al.[23] One milligram Cy3 dye was reconstituted in 1 mL of 0.1 M sodium bicarbonate (pH 9.3). Labeling was performed by conjugating Cy3 dye to Ad37 at a concentration of 10^{12} Ad particles/mL, where reconstituted Cy3 dye was 20% of the final solution. The mixture was allowed to incubate for 30 minutes in the dark with gentle mixing every 10 minutes, followed by overnight dialysis to remove the excess Cy3 dye. The dye-capsomere ratio was calculated by measuring absorbance at 552 nm. One microliter of this Cy3-labeled Ad37 or equal amount of 20% solution of Cy3 dye by itself was injected into the corneal stroma of mice ($n = 4$ per time point per group). Mice were euthanized at the indicated time points. Afterward, corneas were harvested and fixed with 4% paraformaldehyde for 30 minutes in the dark in preparation for confocal microscopy.

ELISA

Untouched, buffer-injected, and Ad37-injected (10^5 TCID) C57BL/6J mouse corneas were removed at indicated time points ($n = 3$ per time point per group) and flash frozen in liquid nitrogen. Corneas were then homogenized in 400 μL of PBS with 1 mM phenylmethylsulfonyl fluoride (PMSF), 1 μg/mL aprotinin, and 10 μg/mL leupeptin (Sigma-Aldrich, St. Louis, MO). The lysates were centrifuged at 10,000*g* for 10 minutes at 4°C, and the supernatants used undiluted for ELISA. KC and MCP-1 protein detection was performed with commercially available sandwich ELISA kits with capture and detection antibodies, according to the manufacturer's instructions (R&D Systems, Minneapolis, MN). Each sample and standard was analyzed in duplicate. The plates were read on a microplate reader (Molecular Devices, Sunnyvale, CA) and analyzed (SOFTmax software; Molecular Devices). For the myeloperoxidase (MPO) assay, MPO levels were determined by sandwich ELISA according to the manufacturer's protocol (Cell Sciences, Canton, MA). Three corneas each from buffer or Ad37-injected mice were homogenized in 350 μL of lysis buffer (200 mM NaCl, 5 mM EDTA, 10 mM Tris-HCl, 10% glycine, 1 mM PMSF, 1 μg/mL leupeptin, and 10 μg/mL aprotinin) and centrifuged at 1000*g* for 10 minutes at 4°C, and the

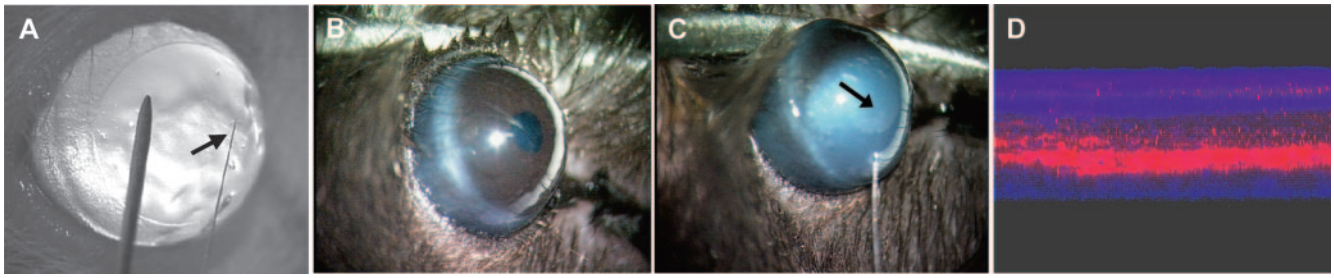

FIGURE 1. The mouse corneal stroma was injected with virus-free dialysis buffer or Ad37 by a gas-powered microinjection system and a capillary glass needle. (**A**) Comparison showing a 33-gauge needle and a glass micropipette needle (*arrow*) on the background of a BALB/c mouse cornea. (**B**) Uninjected eye of C57BL/6J mouse (**C**) Intrastromal injection caused immediate clouding of mouse cornea. *Arrow*: distal tip of the glass needle in the center of cornea. (**D**) Composite confocal image taken immediately after injection showing successful injection of Cy3-labeled Ad37 (*red*) in the center of mouse corneal stroma. Nuclei were stained with DAPI (*blue*).

supernatants collected for the assay. Each sample and the standards provided were analyzed in duplicate.

Histopathology and Immunohistochemistry

Mouse corneas injected with buffer or Ad37 were removed, rinsed in PBS, and fixed with 10% neutral buffered formalin for 24 hours at room temperature. After paraffin embedding, whole eyes were cut into 5-μm-thick sections, mounted on positively charged slides and air dried overnight. After deparaffinization and rehydration, slides were stained with hematoxylin and eosin or treated with 0.01 M citrate buffer (Biopath, Oklahoma City, OK) for epitope retrieval and immunohistochemistry. Nonspecific binding was blocked using protein block (Dako, Carpinteria, CA) supplemented with Fc block (CD16/CD32; BD-Pharmingen, San Diego, CA) and 5% rat serum (Jackson ImmunoResearch Laboratories, West Grove, PA). The slides were incubated with primary antibody against MPO (Neomarkers, Fremont, CA), or neutrophils (Serotec, Oxford, UK) for 30 minutes. Immunodetection was performed with biotin-streptavidin and alkaline phosphatase according to the manufacturer's instructions (Biopath). Slides were counterstained with hematoxylin, coverslipped using a synthetic resin, and photographed (Axiovert 135; Carl Zeiss Meditec, Inc.), using a 40× objective.

Confocal Microscopy

Mice corneas injected with buffer or Ad37 were removed at indicated time points after injection and fixed in 4% paraformaldehyde for 30 minutes at room temperature. Nonspecific binding was blocked by PBS supplemented with 4% bovine serum albumin, 0.25% gelatin, 0.1% Triton X-100, 5% rat serum, and 1:100 Fc block for 4 hours at 4°C. The corneas were then incubated in fluorescein isothiocyanate (FITC)-labeled primary antibodies against Ly6G (Serotec) or F4/80 (Serotec) overnight at 4°C. FITC-labeled IgG2b (Serotec) was used as the isotype control. After they were washed with PBS, corneas were flatmounted on coverslips with mounting medium containing DAPI (4,6-diamidino-2-phenylindole; Vectashield; Vector Laboratories, Burlingame, CA). Five radial incisions were made to facilitate flattening of each cornea. Corneas were scanned in the *z*-axis with a step size of 1 to 2 μm with an confocal laser scanning microscope (IX81-FV500; Olympus, Melville, NY) equipped with a 40× water immersion objective lens. The microscope system software (FluoView; Olympus) was used for analysis.

Statistical Analysis

Real-time PCR and ELISA experiments for chemokine expression were each performed three times. Mean values from three experiments were compared by ANOVA with the Scheffé multiple comparison test. Statistical significance was set at $\alpha = 0.05$. The MPO ELISA was performed three times, and the data were analyzed by Student's *t*-test.

RESULTS

Experimental Adenovirus Keratitis

Glass pipette needles (Fig. 1A, arrow) and a gas-powered microinjection system were used to inject 1 μL of virus-free dialysis buffer or Ad37 into the stroma of C57BL/6J mouse corneas under an ophthalmic surgical microscope. Figure 1B shows an uninjected eye. Successful injection into the corneal stroma was indicated by immediate clouding of the cornea (Fig. 1C). This clouding resolved within 20 to 30 minutes after injection (data not shown). A composite confocal image taken immediately after a successful injection of Cy3-labeled Ad37 in the center of mouse corneal stroma is shown in Figure 1D.

Virus-free dialysis buffer or Ad37 at 10^1 to 10^5 TCID was then used to determine whether Ad37 would induce keratitis in the C57BL/6J mouse. Mouse eyes were examined for inflammation every day for 4 days after injection and then were euthanatized for histopathological examination. Buffer- or 10^1, 10^2, or 10^3 TCID–injected mice did not demonstrate clinical signs of inflammation within the first 4 days after injection by examination of live anesthetized mice under a surgical operating microscope or any inflammatory cells by histopathology (Figs. 2A–H). Injection of 10^4 TCID of Ad37 induced subtle and inconsistent signs of inflammation clinically (Fig. 2I). Histopathological sections on 10^4 TCID-injected corneas also showed very few inflammatory cells (Fig. 2J) and these were not present in every cornea (data not shown). By clinical examination, corneal injection of 10^5 TCID of Ad37 in C57BL/6J mice induced keratitis in all animals (Fig. 2K). Histopathology showed inflammatory cells throughout the corneal stroma (Fig. 2L). Collagen fiber separation in the corneal stroma and thinning and flattening of the corneal epithelium was also seen. Inflammatory cells occasionally formed subepithelial infiltrates (Fig. 2L, arrows).

C57BL/6J mice injected with 10^5 TCID of Ad37 or virus-free dialysis buffer were also examined and photographed daily for a week and then weekly for 3 months. Buffer-injected eyes did not show clinical signs of inflammation at any time after injection (Figs. 3A, C, E, G). Ad37-injected eyes showed observable corneal opacities as early as 1 day after injection (Fig. 3B). Corneal opacity reached a peak by 4 days after injection, at which time the opacity typically spanned over half the corneal surface diameter (Fig. 3D). The opacity then persisted for several weeks, gradually decreasing in size (Fig. 3F). Occasional subepithelial opacities were observed at later time points (Fig. 3H, arrows). The complete resolution of all opacities was usually evident within 2 to 3 months after injection (data not shown).

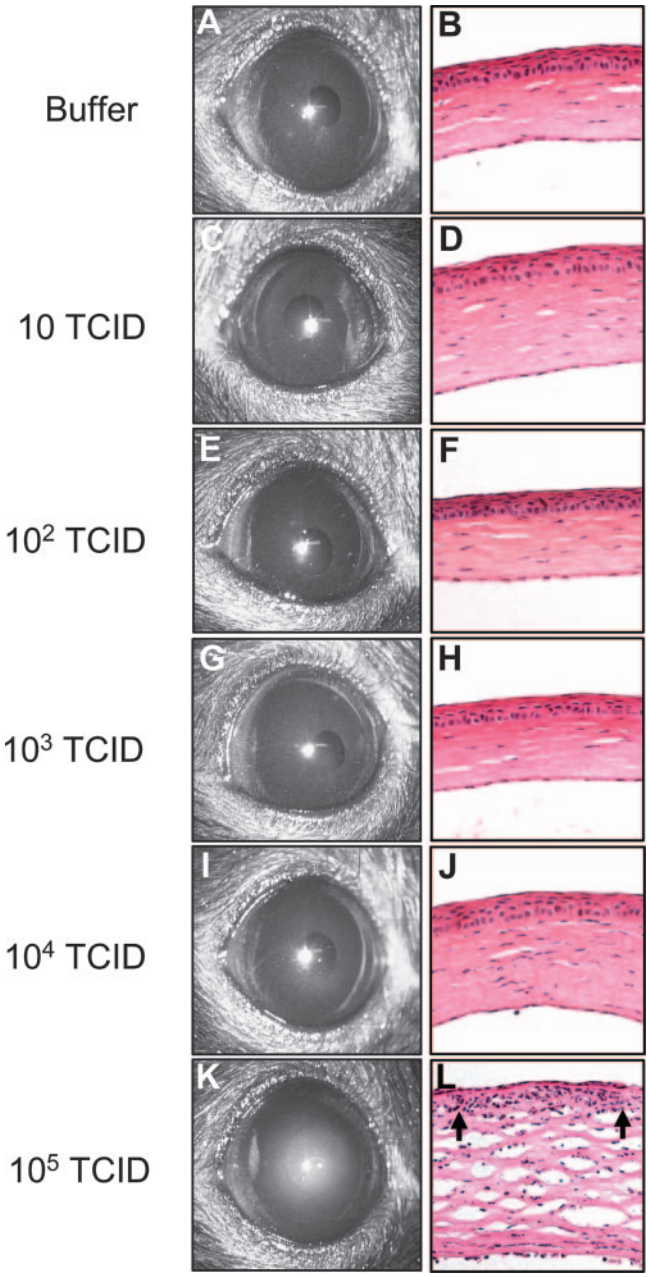

FIGURE 2. Representative clinical photographs and hematoxylin-eosin–stained sections of mouse corneas at 4 days after injection with different doses of Ad37 (10^1–10^5 TCID; $n = 5$ mice/group). (**A**–**H**) Injection of 10^1 to 10^3 TCID of Ad37 did not cause inflammation based on either clinical examination or histopathology. Injection of 10^4 TCID of Ad37 induced subtle and inconsistent signs of inflammation on clinical examination (**I**) and histopathology (**J**). Gross examination of 10^5 TCID injected mice revealed central opacities in all corneas (**K**). Histopathology revealed a characteristic subepithelial infiltrate (**L**, *arrows*).

Ad37 Entry and Intracellular Trafficking

To determine whether Ad37 enters resident corneal cells of C57BL/6J mice, we labeled Ad37 with Cy3 fluorescent dye and followed its progress using confocal microscopy at 0, 10, 30, and 90 minutes after injection (Fig. 4). Control corneal injections with virus-free Cy3 dye were also performed and observed at the same time points. Immediately after injection, Ad37 was seen distributed within the central corneal stroma (Fig. 4A). At 10 minutes after injection, Ad37 appeared to bind stromal cell membranes (Fig. 4B). At 30 minutes after injection, Cy3-labeled Ad37 was also seen throughout the cytoplasm (Fig. 4C). At 90 minutes after injection, dye was mostly visible in the perinuclear regions (Fig. 4D). Control injections with virus-free Cy3 dye did not show any fluorescence in the cornea at 10, 30, or 90 minutes after injection (data not shown).

Viral Gene Expression and Replication

We analyzed adenoviral early (E1A 10S and E1B 19k) and late (IIIa) gene expression[24] in the Ad37-injected cornea as an assay to determine viral entry and delivery of viral genome into corneal cell nuclei. Viral gene expression studies were performed with real-time PCR at 4 hours, 1 day, and 4 days after injection. Messenger RNA for both early genes (E1A 10S and E1B 19k) was expressed in the Ad37-injected corneas at 4 hours and 1 day, but fell markedly by 4 days after injection (Fig. 5A). Late gene IIIa transcripts were undetectable at any time point (data not shown).

Next, to analyze viral replication in vivo, Ad37-injected corneas were assayed by viral titer daily for 4 days after injec-

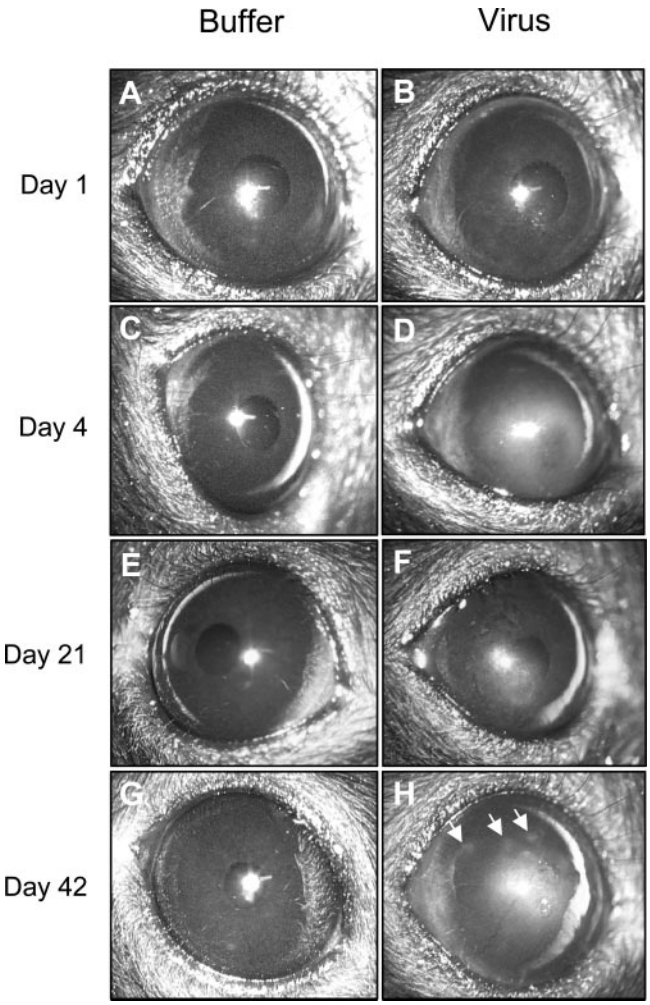

FIGURE 3. Clinical appearance of C57BL/6J mouse eyes injected with dialysis buffer or 10^5 TCID Ad37 ($n = 6$ mice/group). Buffer-injected corneas remained clear at all times after injection (**A**, **C**, **E**, **G**). Opacities in Ad37-injected corneas were seen as early as 1 day after injection (**B**) and appeared to peak at 4 days (**D**). The opacities then regressed slowly (**F**) but sometimes recurred with characteristic subepithelial infiltrates (**H**, *arrows*).

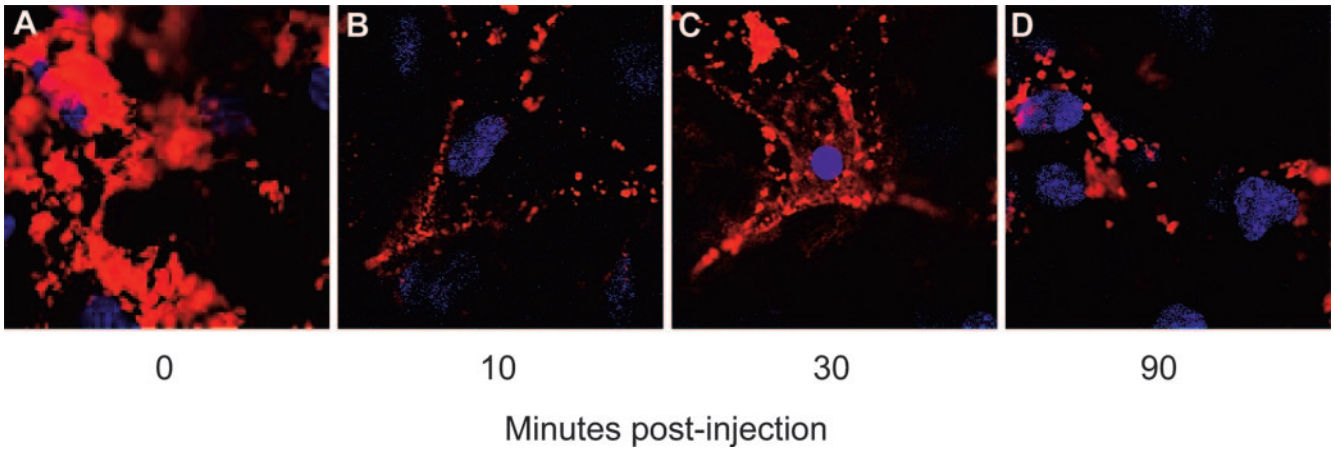

FIGURE 4. Cy3-labeled Ad37 (*red*) was injected into the stroma of C57BL/6J mouse corneas ($n = 4$ mice/time point) and observed by confocal microscopy at various times after injection. (**A**) Immediately after injection, Cy3-labeled Ad37 was seen as a focal collection at the injection site. (**B**) At 10 minutes after injection, the dye appeared to delineate individual cell membranes. (**C**) At 30 minutes, dye was also seen within the cytoplasm, suggesting viral transit into the cell. (**D**) At 90 minutes, dye appeared to coalesce at the perinuclear regions of individual cells. Nuclei were stained with DAPI (*blue*).

tion. Ad37 titers fell gradually from the injected amount (10^5 TCID/cornea) and had declined to approximately 10^3 TCID/cornea by day 4 after injection (Fig. 5B).

Cytokine Expression

Earlier in vitro experiments using human keratocytes and Ad19 showed upregulation of IL-8 and MCP-1 within several hours of infection.[12,19] Published studies of human adenovirus infection of nonocular sites in the mouse showed upregulation of KC, IL-6, IL-1β, and MIP-2.[25,26] To determine changes in cytokine expression in the Ad37-injected mouse corneas, we performed real-time PCR at 4 hours, and ELISA at 0, 8, and 16 hours after injection. By real-time PCR, mRNA expression levels of IL-6, KC, and MCP-1 in Ad37-injected corneas were all significantly greater compared with untouched or buffer-injected corneas at 4 hours after injection (Fig. 6A; $P < 0.05$). By ELISA, KC protein levels were significantly upregulated in Ad37-injected corneas at 8 and 16 hours after injection compared with buffer-injected corneas (Fig. 6B; 21.48 ± 8.94 vs. 4.49 ± 3.78 pg/cornea at 8 hours after injection, 26.82 ± 8.59 vs. 2.45 ± 2.11 pg/cornea at 16 hours after injection, $P < 0.05$). MCP-1 protein levels were significantly upregulated only at 16 hours after injection (Fig. 6C; 157.38 ± 33.33 vs. 25.79 ± 11.96 pg/cornea, $P < 0.05$).

Phenotype of Infiltrating Cells

The acute inflammatory response to human adenoviral infection in EKC is characterized by infiltration by polymorphonuclear neutrophils.[27] To characterize the infiltrating cells in the C57BL/6J mouse corneas infected with Ad37, we performed immunohistochemistry on corneal tissue sections after infection. Analysis of corneas at 4 days after injection with buffer or Ad37 by immunohistochemical staining with anti-neutrophil and anti-MPO antibodies showed reactivity for each antibody only in Ad37-injected corneas (Fig. 7A).

To quantify the levels of induced MPO, we performed an ELISA at 4 days after injection. Corneas injected with 10^5 TCID of Ad37 showed significantly higher levels of MPO compared with buffer injection (Fig. 7B; 30.92 ± 2.6 vs. 0.32 ± 0.03 ng/cornea, $P = 0.0024$). The injection of a lesser dose of Ad37 (5×10^2 TCID) did not induce an elevation of MPO (data not shown).

We then analyzed the phenotype of infiltrating cells in buffer or Ad37-injected C57BL/6J mouse corneas at 4 and 8

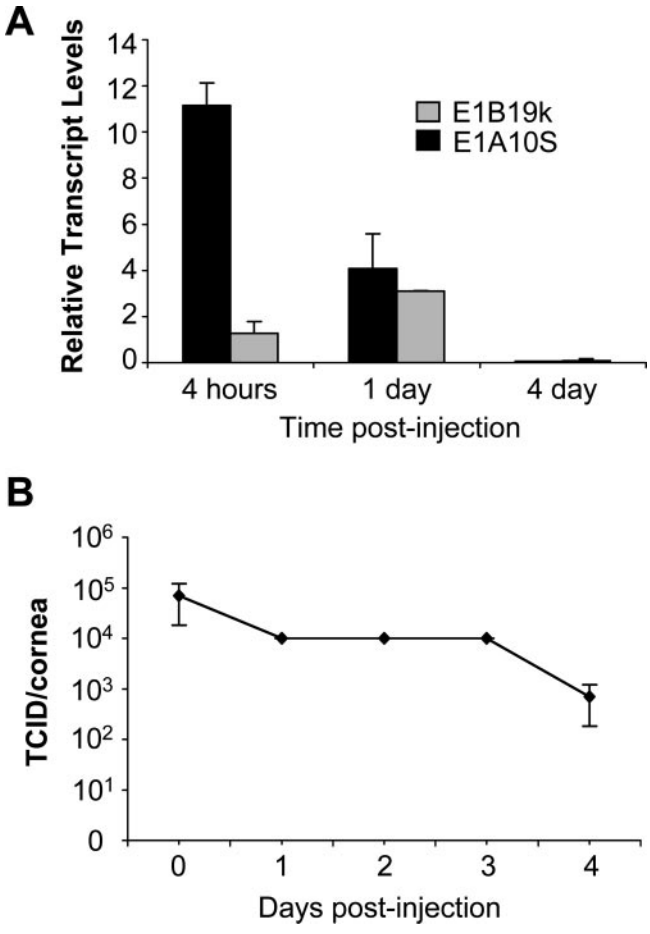

FIGURE 5. mRNA expression (**A**) of viral genes in mouse corneas injected with 10^5 TCID of Ad37 at 4 hours, 1 day, and 4 days after injection. Total RNA was isolated and viral mRNA expression analyzed by real-time PCR. Adenovirus early genes E1A 10S and E1B 19k show highest expression at 4 hours after injection, dropping sharply by day 4. The data shown represent the mean ± SD of results in two separate experiments ($n = 3$/timepoint). (**B**) Ad37 (10^5 TCID) was injected into each mouse cornea and viral replication was analyzed for corneas harvested immediately after injection and daily thereafter for 4 days. The viral titer dropped to 10^3 TCID by 4 days after injection. The values shown represent the mean ± SD of viral titers ($n = 4$/timepoint).

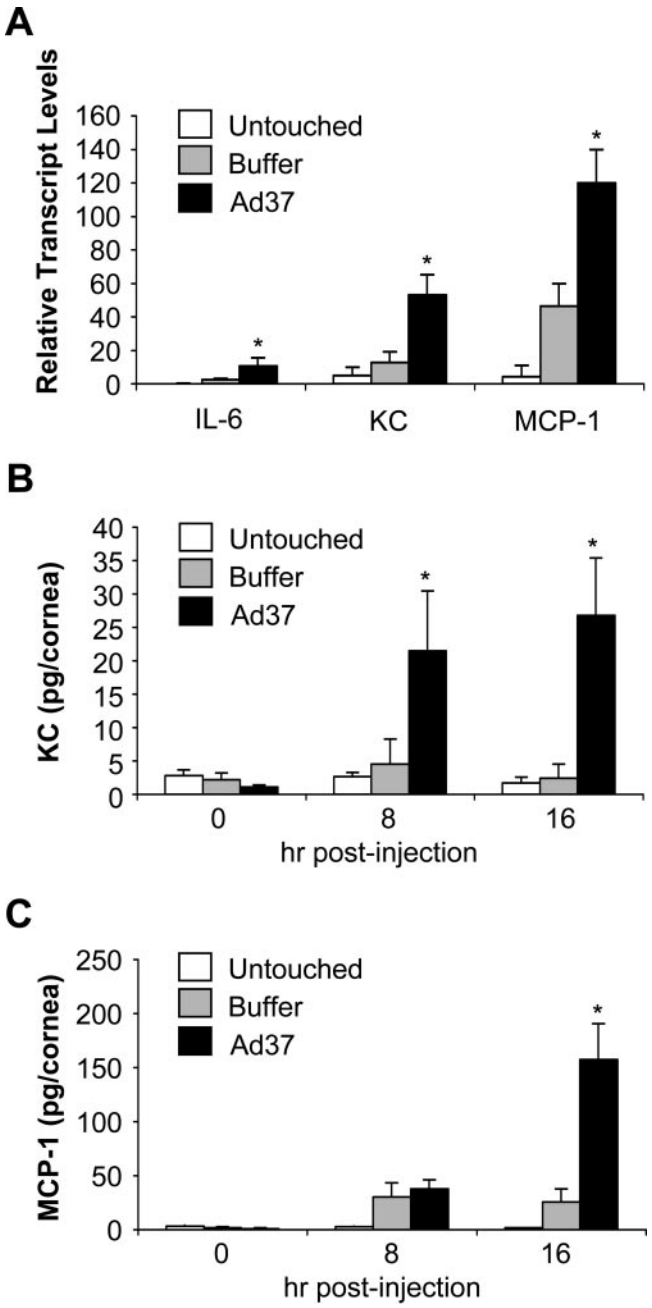

FIGURE 6. Messenger RNA expression (**A**) of cytokines in untouched, buffer, or Ad37-injected (10^5 TCID) corneas at 4 hours after injection. Total RNA was isolated from injected corneas and analyzed by real-time PCR. Ad37-injected corneas showed significantly higher expression of IL-6, KC, and MCP-1 when compared with untouched and buffer-injected corneas. ELISA for (**B**) KC and (**C**) MCP-1 proteins in untouched, buffer, and Ad37-injected (10^5 TCID) C57BL/6J mouse corneas at 0, 8, and 16 hours after injection. Ad37-injected corneas showed significantly higher expression of KC protein at 8 and 16 hours, and MCP-1 protein at 16 hours after injection, when compared to untouched and buffer-injected corneas. The data represent mean ± SD of results in three separate experiments ($n = 3$/time point/group; $^*P < 0.05$).

days after injection by confocal microscopy. We stained corneal wholemounts with FITC-labeled antibodies against Ly6G for neutrophils,[28] F4/80 for macrophages,[29] or an isotype-matched IgG2b antibody. Buffer-injected corneas did not show staining with any of these antibodies (Figs. 8A, 8D, 8G). Ad37-injected corneas showed Ly6G-positive cells predominantly in the anterior stroma (Figs. 8B, 8C). Ad37-injected corneas also contained F4/80-positive cells in the corneal stroma at 4 days after injection, but these were evident only in the peripheral cornea (Figs. 8E, 8F). Sections from corneas taken later in the infection (8 days after injection) showed some F4/80-positive cells at the center of the cornea (data not shown). Isotype IgG2b did not show reactivity in any of the tissue sections examined (Figs. 8G–I).

DISCUSSION

Natural human ocular infection with adenoviruses starts with virus entry and replication in ocular surface epithelial cells. According to the hypothesis of Jones,[30] subsequent corneal subepithelial infiltrates develop as an antigen–antibody reaction to adenoviral antigens soaked up by the anterior stroma after corneal epithelial infection. We have suggested that corneal subepithelial infiltrates occur subsequent to chemokine expression by infected corneal stromal cells.[12,14,19] Histopathology in two human cases identified these opacities as subepithelial collections of mononuclear cells in the anterior corneal stroma, but in both cases the opacities were long

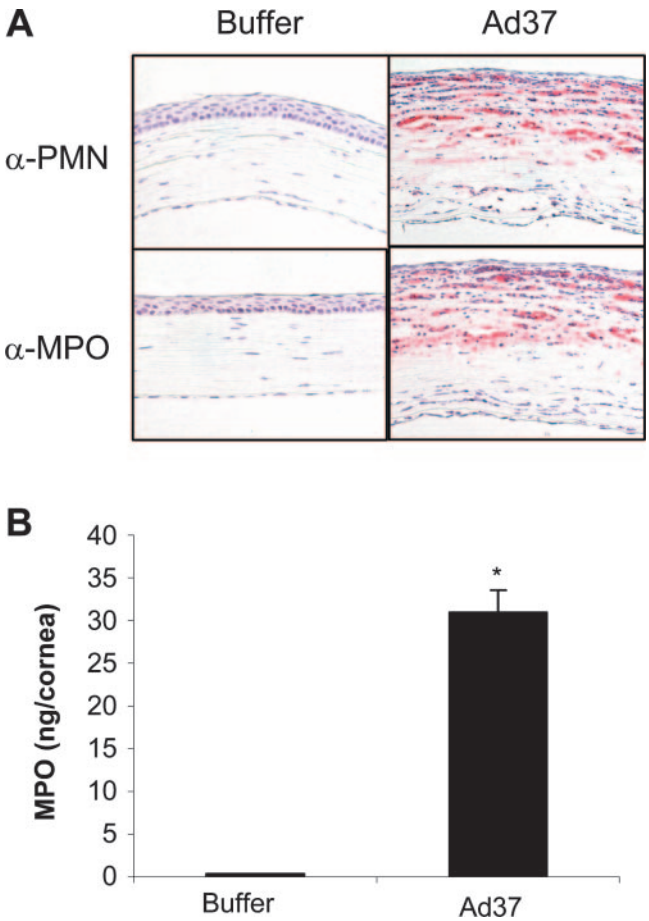

FIGURE 7. Representative immunohistochemical tissue sections comparing Ad37 (10^5 TCID) and buffer-injected corneas ($n = 5$ mice/group) using anti-neutrophil (PMN) and anti-MPO antibodies. Both antibodies showed reactivity in Ad37-injected corneas only. MPO assay (**B**) performed on buffer and Ad37-injected (10^5 TCID) corneas at 4 days after injection ($n = 3$/group). Ad37-injected corneas showed significantly increased levels of MPO when compared to buffer-injected corneas. The values shown represent mean ± SD for three separate experiments ($^*P = 0.0024$).

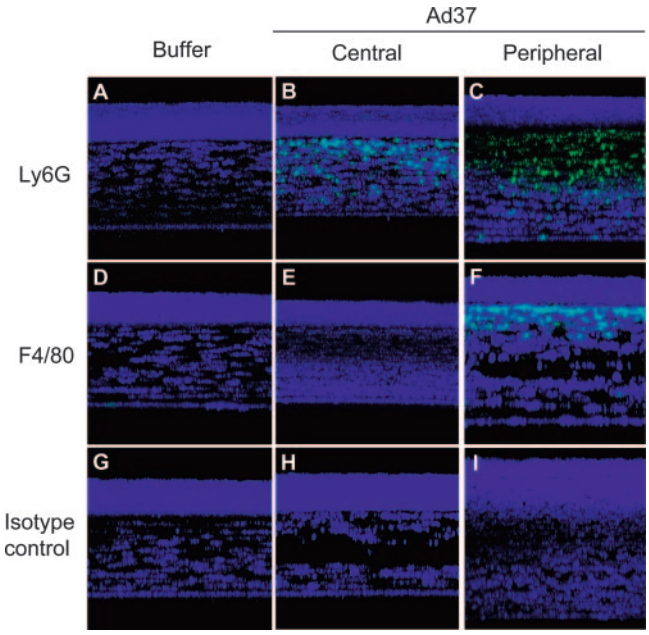

FIGURE 8. Representative composite confocal images of corneal wholemounts at 4 days after stromal injection with buffer or 10^5 TCID Ad37 ($n = 3$ mice/group), using FITC-labeled antibodies against Ly6G, F4/80, and a FITC-labeled isotype control IgG2b. No staining was observed in buffer-injected animals (**A**, **D**, **G**). Corneas injected with Ad37 showed Ly6G positive cells in the central and peripheral corneal stroma (**B**, **C**, respectively). At 4 days after injection, F4/80-positive cells were seen only in the peripheral (**F**) but not in the central corneal stroma (**E**). Isotype control antibody did not show staining (**G**, **H**, **I**). Nuclei are stained with DAPI (*blue*).

standing.[31,32] The pathogenesis and formation of adenoviral subepithelial infiltrates has not been adequately investigated in vivo because of the lack of a suitable animal model.

Topical application of Ad37 to the C57BL/6J mouse cornea with or without prior scarification does not result in keratitis (Chodosh J, unpublished data, 2003). A similar dichotomy is present in rabbits in which adenoviral stromal keratitis does not occur unless the virus is also injected intrastromally.[21] To reduce background inflammation soon after infection, we applied a novel and relatively atraumatic means of corneal stromal injection, effectively bypassing the corneal epithelial cell layer. This overcomes the requirement for precedent viral replication in the nonpermissive mouse corneal epithelium.

Ginsberg et al.[26] described a mouse model of adenoviral pneumonia in C57BL/6N mice using high titers of Ad5 (10^{10} plaque forming units). Trousdale et al.[13] and Gordon et al.[21] both used a relatively high dose of adenovirus (10^6 and 4×10^5 plaque forming units, respectively) to induce subepithelial corneal opacities in rabbits. Similarly, we observed in our mouse model that 10^5 TCID of Ad37 was necessary to produce keratitis reproducibly in all mice injected. A recently published study using adenovirus vectors in mouse brain demonstrated that a threshold infective dose is essential for cytokine expression.[33] The reason for this threshold infective dose is not known. Clearly, a threshold amount of chemokine must be produced for effective chemotaxis of inflammatory cells.[34]

When injected with 10^5 TCID Ad37, diffuse central corneal opacity appeared at 1 day after injection and peaked at 4 days after injection. The diffuse pattern of inflammation most commonly observed in our mouse keratitis model differs from that in human EKC, in which small, multifocal subepithelial infiltrates are characteristic. In humans with EKC, viral interaction with keratocytes may be limited to the superficial stroma after cytopathic infection of the corneal epithelium. We speculate that the relatively diffuse inflammation in our model compared with the multifocal subepithelial infiltrates in humans with EKC results from the more diffuse and widespread interaction between corneal stromal cells and virus after intrastromal injection.

No viral particles, viral antigens, or viral replication were observed in corneas from patients with chronic EKC.[31,32] In our study, Ad37 entry and early gene expression were shown to occur in corneal cells, but not viral replication. The absence of adenoviral replication was not surprising considering the relative nonpermissiveness of mouse cells to adenovirus infection seen by others both in vitro and in vivo.[26,35–37] Replication-deficient adenoviruses have been shown to induce inflammation in a variety of animal models, providing that a relatively high titer of adenovirus was used.[10,11,13,38] These studies suggest that inflammation in adenoviral infection may result at least in part from virus capsid interactions with target cells rather than viral gene expression and replication. The integrin $\alpha v\beta 5$ is known to be a secondary receptor used by adenoviruses,[39] and integrin β_5 is expressed in the mouse corneal stroma.[40] The detection of adenoviral early gene transcripts leaves open the possibility that viral genes contributed to corneal stromal inflammation in our mouse model.[41,42]

Neutrophils were the first cells seen in the corneal stroma of Ad37-injected mice. We observed mononuclear cells later in the infection, and they were fewer in number. KC is a murine homologue of the human chemokine Gro-α, binds to murine IL-8 receptor type B homologue, and is thought to be a major chemotactic molecule for neutrophils in mice.[43,44] MCP-1 is chemotactic for mononuclear cells.[45] We observed expression of both KC and MCP-1 in our animal model within hours after injection of 10^5 TCID of Ad37. The kinetics of chemokine expression in our animal model seems to correlate with the infiltrating immune cells. KC is expressed first, followed by expression of MCP-1. Similar kinetics of chemokine expression and infiltrating cells have been shown in mouse corneas in response to IL-1β.[46] Whether KC and MCP-1 are solely responsible for infiltration of neutrophils and monocytes in adenovirus keratitis or redundant in their action remains to be explored.

The cells and molecular mechanisms responsible for rapid expression of chemokines in the mouse model of Ad37 keratitis are not clear at present. In vitro experiments have shown that Ad19 binding to human keratocytes activates MAP kinases within minutes of the interaction, with subsequent kinase activity necessary for expression of IL-8 and MCP-1.[12,19] Based on other studies,[14,17,47] we speculate that resident keratocytes in the mouse play a major role in the keratitis induced by Ad37 infection. Considering the kinetics of chemokines and infiltrating cells, we hypothesize that activation of signaling pathways by binding of virus to keratocytes induces the expression of KC and MCP-1 and subsequent leukocyte infiltration. Use of this new mouse model of adenovirus keratitis will allow us to investigate this and other hypotheses regarding the immunopathogenesis of adenovirus keratitis.

Acknowledgments

Authors thank Mark Dittmar, Louisa Williams, and Linda Boone for technical assistance.

References

1. Rowe WP, Heubner RJ, Gilmore LK, Parrott RH, Ward TG. Isolation of a cytopathogenic agent from human adenoids undergoing spontaneous degeneration in tissue culture. *Proc Soc Exp Biol Med.* 1953;84:570–573.

2. Hilleman MR, Werner JH. Recovery of new agent from patients with acute respiratory illness. *Proc Soc Exp Biol Med*. 1954;85: 183–188.
3. Russell WC, Benko M. Adenoviruses (*Adenoviridae*): animal viruses. In: Webster RG, Granoff A, eds. *Encyclopedia of Virology,* London: Academic Press; 1999:14–21.
4. Jogler C, Hoffmann D, Theegarten D, Grunwald T, Uberla K, Wildner O. Replication properties of human adenovirus in vivo and in cultures of primary cells from different animal species. *J Virol*. 2006;80:3549–3558.
5. Lukashok SA, Horwitz MS. New perspectives in adenoviruses. *Curr Clin Top Infect Dis*. 1998;18:286–305.
6. Kojaoghlanian T, Flomenberg P, Horwitz MS. The impact of adenovirus infection on the immunocompromised host. *Rev Med Virol*. 2003;13:155–171.
7. Kemp MC, Hierholzer JC, Cabradilla CP, Obijeski JF. The changing etiology of epidemic keratoconjunctivitis: antigenic and restriction enzyme analyses of adenovirus types 19 and 37 isolated over a 10-year period. *J Infect Dis*. 1983;148:24–33.
8. Butt AL, Chodosh J. Adenoviral keratoconjunctivitis in a tertiary care eye clinic. *Cornea*. 2006;25:199–202.
9. Ford E, Nelson KE, Warren D. Epidemiology of epidemic keratoconjunctivitis. *Epidemiol Rev*. 1987;9:244–261.
10. Kafri T, Morgan D, Krahl T, Sarvetnick N, Sherman L, Verma I. Cellular immune response to adenoviral vector infected cells does not require de novo viral gene expression: implications for gene therapy. *Proc Natl Acad Sci USA*. 1998;95:11377–11382.
11. McCoy RD, Davidson BL, Roessler BJ, et al. Pulmonary inflammation induced by incomplete or inactivated adenoviral particles. *Hum Gene Ther*. 1995;6:1553–1560.
12. Natarajan K, Rajala MS, Chodosh J. Corneal IL-8 expression following adenovirus infection is mediated by c-Src activation in human corneal fibroblasts. *J Immunol*. 2003;170:6234–6243.
13. Trousdale MD, Nobrega R, Wood RL, et al. Studies of adenovirus-induced eye disease in the rabbit model. *Invest Ophthalmol Vis Sci*. 1995;36:2740–2748.
14. Chodosh J, Astley RA, Butler MG, Kennedy RC. Adenovirus keratitis: a role for interleukin-8. *Invest Ophthalmol Vis Sci*. 2000; 41:783–789.
15. Cubitt CL, Lausch RN, Oakes JE. Differential induction of GRO alpha gene expression in human corneal epithelial cells and keratocytes exposed to proinflammatory cytokines. *Invest Ophthalmol Vis Sci*. 1997;38:1149–1158.
16. Cubitt CL, Lausch RN, Oakes JE. Differences in interleukin-6 gene expression between cultured human corneal epithelial cells and keratocytes. *Invest Ophthalmol Vis Sci*. 1995;36:330–336.
17. Hong JW, Liu JJ, Lee JS, et al. Proinflammatory chemokine induction in keratocytes and inflammatory cell infiltration into the cornea. *Invest Ophthalmol Vis Sci*. 2001;42:2795–2803.
18. Tran MT, Tellaetxe-Isusi M, Elner V, Strieter RM, Lausch RN, Oakes JE. Proinflammatory cytokines induce RANTES and MCP-1 synthesis in human corneal keratocytes but not in corneal epithelial cells: beta-chemokine synthesis in corneal cells. *Invest Ophthalmol Vis Sci*. 1996;37:987–996.
19. Xiao J, Chodosh J. JNK regulates MCP-1 expression in adenovirus type 19-infected human corneal fibroblasts. *Invest Ophthalmol Vis Sci*. 2005;46:3777–3782.
20. Tsai JC, Garlinghouse G, McDonnell PJ, Trousdale MD. An experimental animal model of adenovirus-induced ocular disease: the cotton rat. *Arch Ophthalmol*. 1992;110:1167–1170.
21. Gordon YJ, Romanowski E, Araullo-Cruz T. An ocular model of adenovirus type 5 infection in the NZ rabbit. *Invest Ophthalmol Vis Sci*. 1992;33:574–580.
22. De Hauwere B, Lutz A, Maudgal PC, Neyts J, de Clercq E. An ocular model of adenovirus type 5 infection in the rabbit. *Bull Soc Belge Ophtalmol*. 1995;259:33–42.
23. Leopold PL, Ferris B, Grinberg I, Worgall S, Hackett NR, Crystal RG. Fluorescent virions: dynamic tracking of the pathway of adenoviral gene transfer vectors in living cells. *Hum Gene Ther*. 1998;9:367–378.
24. Shenk, T. Adenoviridae: the viruses and their replication. In: Fields BN, Knipe DM, Howley PM, ed. *Virology.* Vol. 2. Philadelphia: Lippincott-Raven; 1996:2111–2148.
25. Kajon AE, Gigliotti AP, Harrod KS. Acute inflammatory response and remodeling of airway epithelium after subspecies B1 human adenovirus infection of the mouse lower respiratory tract. *J Med Virol*. 2003;71:233–244.
26. Ginsberg HS, Moldawer LL, Sehgal PB, et al. A mouse model for investigating the molecular pathogenesis of adenovirus pneumonia. *Proc Natl Acad Sci USA*. 1991;88:1651–1655.
27. Jones DB. Viral and chlamydial keratoconjunctivitis. In: *Symposium on Medical and Surgical Diseases of Cornea. Transactions of the New Orleans Academy of Ophthalmology*. St. Louis: CV Mosby; 1980;497–523.
28. Hestdal K, Ruscetti FW, Ihle JN, et al. Characterization and regulation of RB6–8C5 antigen expression on murine bone marrow cells. *J Immunol*. 1991;147:22–28.
29. Hirsch S, Austyn JM, Gordon S. Expression of the macrophage-specific antigen F4/80 during differentiation of mouse bone marrow cells in culture. *J Exp Med*. 1981;154:713–725.
30. Jones BR. Adenovirus infections of the eye in London. *Trans Ophthalmol Soc UK*. 1962;82:621–640.
31. Lund OE, Stefani FH. Corneal histology after epidemic keratoconjunctivitis. *Arch Ophthalmol*. 1978;96:2085–2088.
32. Tullo AB, Ridgway AE, Lucas DR, Richmond S. Histopathology of adenovirus type 8 keratitis. *Cornea*. 1987;6:234.
33. Zirger JM, Barcia C, Liu C, et al. Rapid upregulation of interferon-regulated and chemokine mRNAs upon injection of 10^8 international units, but not lower doses, of adenoviral vectors into the brain. *J Virol*. 2006;80:5655–5659.
34. Lin F, Nguyen CM, Wang SJ, Saadi W, Gross SP, Jeon NL. Effective neutrophil chemotaxis is strongly influenced by mean IL-8 concentration. *Biochem Biophys Res Commun*. 2004;319:576–581.
35. Blair GE, Dixon SC, Griffiths SA, Zajdel ME. Restricted replication of human adenovirus type 5 in mouse cell lines. *Virus Res*. 1989; 14:339–346.
36. Silverstein G, Strohl WA. Restricted replication of adenovirus type 2 in mouse BALB/3T3 cells. *Arch Virol*. 1986;87:241–264.
37. Zucker ML, Flint SJ. Infection and transformation of mouse cells by human adenovirus type 2. *Virology*. 1985;147:126–141.
38. Muruve DA, Barnes MJ, Stillman IE, Libermann TA. Adenoviral gene therapy leads to rapid induction of multiple chemokines and acute neutrophil-dependent hepatic injury in vivo. *Hum Gene Ther*. 1999;10:965–976.
39. Wickham TJ, Mathias P, Cheresh DA, Nemerow GR. Integrins alpha v beta 3 and alpha v beta 5 promote adenovirus internalization but not virus attachment. *Cell*. 1993;73:309–319.
40. Zhang H, Li C, Baciu PC. Expression of integrins and MMPs during alkaline-burn-induced corneal angiogenesis. *Invest Ophthalmol Vis Sci*. 2002;43:955–962.
41. Keicho N, Elliott WM, Hogg JC, Hayashi S. Adenovirus E1A upregulates interleukin-8 expression induced by endotoxin in pulmonary epithelial cells. *Am J Physiol*. 1997;272:L1046–L1052.
42. Schaack J. Induction and inhibition of innate inflammatory responses by adenovirus early region proteins. *Viral Immunol*. 2005;18:79–88.
43. Bozic CR, Gerard NP, von Uexkull-Guldenband C, et al. The murine interleukin 8 type B receptor homologue and its ligands: expression and biological characterization. *J Biol Chem*. 1994;269: 29355–29358.
44. Bozic CR, Kolakowski LF Jr, Gerard NP, et al. Expression and biologic characterization of the murine chemokine KC. *J Immunol*. 1995;154:6048–6057.
45. Rollins BJ. Chemokines. *Blood*. 1997;90:909–928.
46. Nakao S, Kuwano T, Tsutsumi-Miyahara C, et al. Infiltration of COX-2-expressing macrophages is a prerequisite for IL-1beta-induced neovascularization and tumor growth. *J Clin Invest*. 2005; 115:2979–2991.
47. Garcia-Ramallo E, Marques T, Prats N, Beleta J, Kunkel SL, Godessart N. Resident cell chemokine expression serves as the major mechanism for leukocyte recruitment during local inflammation. *J Immunol*. 2002;169:6467–6473.